A. J. Richardson
C. L. Wiegand
U. S. Dept. of Agriculture
Weslaco, TX 78596

Distinguishing Vegetation from Soil Background Information*

A gray mapping technique allows delineation of any Landsat scene into vegetative cover stages, degrees of soil brightness, and water.

(Abstract on next page)

Introduction

Efforts to interpret vegetated surface reflectance from aircraft and satellite multispectral scanner (MSS) observations have been hampered by soil background signals that are superimposed on or intermingled with information about vegetation. Soil reflectance varies with soil type, water content, and tillage. Several researchers have shown that Landsat spectral data relate closely with such vegetation density indicators as biomass, leaf area index, percent cover, and plant population on a given date at a given location. Signature extension to several dates (temporally) and several locations (spatially) is still a problem. A procedure that accounts for soil background could contribute considerably to operational use of Landsat and other spectral data to monitor the productivity of range, forest, and crop lands.

Our approach was first to study soil reflectance that supplies the background signal of vegetated surfaces. We assumed that crop and soil condition survey systems that attempt to develop spectral indicators of the seasonal development of vegetation amounts and conditions (Rouse *et al.*, 1973; Deering *et al.*, 1975), plant canopy models for yield estimations (Allen and Richardson, 1968; Suits, 1971; Smith *et al.*, 1973; Wiegand *et al.*, 1974; Richardson *et al.*, 1975; Tucker, 1977), or pattern recognition techniques for acreage surveys of crop and soil conditions would benefit by procedures that account for soil background variations.

Kauth and Thomas (1976) determined that the data space distribution of soil reflectance variation in Landsat data is confined to a line (in two-dimensional data space) or a plane (in three-dimensional data space). Reflectance variation of developing vegetation grows perpendicularly out of this plane of soils. We reasoned that this inherent distribution of soil reflectance in Landsat data space might usefully be applied to better understand the effect of soil background on the spectral indicators of vegetation conditions. Consequently, we investigated the distribution of soil reflectance variation for Landsat MSS data, collected in Hidalgo County, Texas, in order to determine whether it could be used as a reference against which vegetation development could be monitored.

Experimental Procedures

In this study, we used the Landsat data space as recorded on the computer compatible tapes (CCT) received from the EROS data center at Sioux Falls, South Dakota, in order to determine Kauth's (1976) plane of soils.

Landsat-1 and -2 overpasses on April 2, May 17, June 4, July 10, October 17, and December 10, 1975 (scene I.D.'s are 2070-16203, 5028-16113, 5046-16103, 5082-16083, 2268-16190, and 2322-16183, respectively) furnished one set of digital data for this study. These scenes were chosen because they encompassed a test county where ground truth was available, and they were sufficiently cloud-free to use. Mean digital values for all four multispectral scanner (MSS) bands, MSS4 (0.5 to 0.6 μm), MSS5

* Contribution from the Soil and Water Conservation Research, Southern Region, Agricultural Research Service, USDA. This study was supported in part by the National Aeronautics and Space Administration under Contract No. T-4105B.

Photogrammetric Engineering and Remote Sensing,
Vol. 43, No. 12, December 1977, pp. 1541-1552.

(0.6 to 0.7 μm), MSS6 (0.7 to 0.8 μm), and MSS7 (0.8 to 1.1 μm), were extracted from the CCT for water, cloud tops, cloud shadows, and high and low reflecting soil in ground-truthed land areas on each overpass date. Sun elevation above the horizon was also obtained from the CCT. A linear correlation analysis between MSS5 and MSS7 was conducted on these data.

A second data set was comprised of mean digital values for sorghum fields at various maturity stages that were extracted from the April 2, May 17, May 26, and June 4, 1975 Landsat CCT for dry and irrigated cropland study sites. Sorghum LAI data (Allen and Richardson, 1968; Wiegand et al., 1974) were collected on May 6 and June 3, 1975 for the dry cropland study sites and on April 24 and May 24, 1975 for the irrigated cropland study sites. These ground truth (GT) data were used to document sorghum development for comparison with the MSS data.

A third data set comprised of sorghum Landsat-1 digital data collected May 27, 1973 and corresponding LAI measurements, previously reported by Richardson *et al.* (1975), were compared with results for 1975.

ABSTRACT: *Landsat-1 and -2 multispectral scanner (MSS) data from six overpass dates (April 2, May 17, June 4, July 10, October 17, and December 10, 1975) showed that MSS digital data for bare soil, cloud tops, and cloud shadows followed a highly predictable linear relation (soil background line) for MSS bands 5 and 7 (r^2=0.974) and bands 5 and 6 (r^2=0.986). Increasing vegetation development, documented by leaf area index (LAI) measurements, for 1973 and 1975 grain sorghum crops, was associated with displacement of sorghum MSS digital counts perpendicularly away from the soil background line. Consequently, the perpendicular distance of a sorghum MSS measurement from the soil background line was tested as an index of plant vegetative development. Two perpendicular vegetation index models, the PVI and PVI6, yielded significant coefficients of determination (r^2) of 0.522 and 0.659, respectively, with LAI.*

Coefficients of determination (r^2) for a transformed vegetation index (TVI6) and a green vegetation index (GVI) that have been used by others were 0.531 and 0.653, respectively, for the same data set. The PVI technique permits the calculation of the coordinates of the intersection of the vegetation and soil background lines; hence, it gives the position of a given pixel on the soil background line that other vegetation indexes do not. Since position along the soil background line should vary with soil water content, soil crusting, and crop shadows, the possibility of deducing information about soil surface conditions becomes apparent.

The Landsat data space surrounding the soil background line for MSS5 and MSS7 was divided into ten decision regions corresponding to water; cloud shadow; low, medium, and high reflecting soil; cloud tops; low, medium, and dense plant cover; and a region (threshold) into which no Landsat data are expected to fall. It was demonstrated that, by using a table lookup procedure and printer symbols for each decision region, Landsat study areas or scenes could be gray mapped to meaningfully display vegetation density and soil condition categories without prior knowledge of local crop and soil conditions.

EXPERIMENTAL RESULTS

SOIL BACKGROUND REFLECTANCE

The Landsat digital data from the first data set (Table 1) for soil, water, and cloud conditions were used to determine Kauth's plane of soils. Digital counts for water, and for high and low reflecting soil, were not determined for May and June 1975 since almost all land areas were cropped. Kauth's plane of soils over six dates was characterized statistically by linear correlation analyses of all possible pairwise combinations for the four MSS

TABLE 1. MEAN DIGITAL COUNTS FROM SIX LANDSAT-1 AND -2 OVERPASSES IN 1975 FOR SOIL, WATER, AND CLOUD CONDITIONS IN HIDALGO AND WILLACY COUNTIES, TEXAS. THE MAXIMUM DIGITAL COUNT FOR LANDSAT MULTISPECTRAL SANNER (MSS) BANDS 4, 5, AND 6 IS 127 AND FOR 7 IT IS 63. THE NUMBER IN PARENTHESIS FOR EACH OVERPASS DATE IS THE SUN ELEVATION.

Soil, water, or atmospheric condition	April 2, 1975 (51°) (Scene I.D. 2070-16203)				May 17, 1975 (57°) (Scene I.D. 5028-16113)				June 4, 1975 (59°) (Scene I.D. 5046-16103)			
	MSS4	MSS5	MSS6	MSS7	MSS4	MSS5	MSS6	MSS7	MSS4	MSS5	MSS6	MSS7
	Digital counts											
High reflecting bare soil	48	68	66	24	—	—	—	—	—	—	—	—
Low reflecting bare soil	26	31	36	15	—	—	—	—	—	—	—	—
Cloud	99	109	111	50	97	96	95	40	127	127	118	55
Cloud shadow	24	24	31	12	38	29	33	12	28	20	21	8
Water	34	32	16	2	—	—	—	—	—	—	—	—

Soil, water, or atmospheric condition	July 10, 1975 (56°) (Scene I.D. 5082-16083)				October 17, 1975 (44°) (Scene I.D. 2268-16190)				December 10, 1975 (32°) (Scene I.D. 2322-16183)			
	MSS4	MSS5	MSS6	MSS7	MSS4	MSS5	MSS6	MSS7	MSS4	MSS5	MSS6	MSS7
	Digital counts											
High reflecting bare soil	77	90	86	34	43	63	70	28	39	58	61	24
Low reflecting bare soil	40	43	40	17	22	30	32	14	14	18	18	7
Cloud	120	120	107	45	—	—	—	—	—	—	—	—
Cloud shadow	32	24	26	11	—	—	—	—	—	—	—	—
Water	40	30	17	4	29	26	12	1	17	15	9	1

bands using 16 digital counts of cloud tops, cloud shadows, and high and low reflecting soil (Table 2). The pairwise band combinations (4, 5) and (6, 7) were not investigated further, because bands within the visible and infrared are known to be highly intercorrelated. Potter and Mendlowitz (1975) showed that the (4, 5) band combination may be useful for determining haze levels of the atmosphere, but we did not include such considerations in the present study. The pairwise band combinations (4, 6) and (4, 7) were not considered because of their lower correlation coefficients and higher standard errors of estimate ($S_{X1 \cdot X2}$) than the band combinations (5, 6) and (5, 7). These latter two combinations were chosen for further study because they have been found useful in the past (Rouse *et al.*, 1973; Wiegand *et al.*, 1974; Deering *et al.*, 1975; Kalensky and

TABLE 2. LINEAR EQUATIONS DETERMINING KAUTH'S LINE OF SOIL FOR ALL POSSIBLE PAIRWISE COMBINATIONS OF THE 4 LANDSAT MSS BANDS. DIGITAL COUNT DATA ARE FOR APRIL 2, MAY 17, JUNE 4, JULY 10, OCTOBER 17, AND DECEMBER 10, 1975 FROM HIGH AND LOW REFLECTING SOIL, AND CLOUD AND CLOUD SHADOWS (N=16).

MSS band pairwise combination (X_1, X_2)	Correlation coefficient (r)	Linear equations $X_1 = a_0 + a_1X_2$	Standard error of estimate ($S_{X1 \cdot X2}$)
			Digital counts
(4 , 5)	0.967	$X_1 = -1.04 + 0.938X_2$	10
(4 , 6)	0.949	$X_1 = -5.45 + 1.011X_2$	12
(4 , 7)	0.958	$X_1 = -1.23 + 2.257X_2$	11
(5 , 6)	0.993	$X_1 = -5.49 + 1.091X_2$	5
(5 , 7)	0.987	$X_1 = -0.01 + 2.400X_2$	6
(6 , 7)	0.993	$X_1 = 5.09 + 2.200X_2$	4

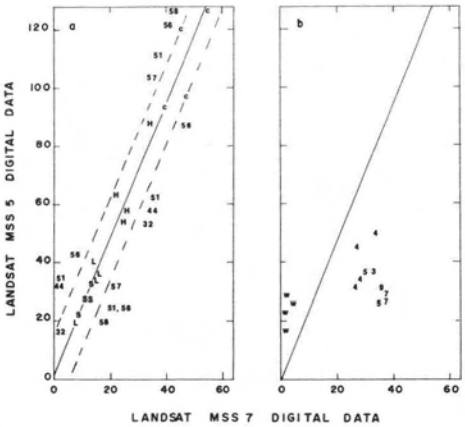

FIG. 1. Scatter diagram of digital data (1) from Landsat bands 5 and 7 for cloud tops (C), cloud shadows (S), high reflecting soil (H), and low reflecting soil (L). Sun elevation for each category was as follows: April 2 (51°), May 17 (57°), June 4 (58°), July 10 (56°), October 17 (44°), and December 10 (32°), 1975. The regression line (MSS5=0.01+ 2.4MSS7) and standard error of estimate ($S_{X1 \cdot X2} = \pm 6$) are plotted as solid and dashed lines, respectively. The coefficient of determination was $r^2 = 0.974$*. Scatter diagram of digital data (b) from Landsat bands 5 and 7 for ten sorghum fields collected on May 27, 1973. Sorghum fields are identified by their LAI value rounded to one digit. Water (W) from four Landsat overpasses, April 2, July 10, October 17, and December 10, 1975, are also plotted. The solid line is the soil background line determined from Figure 1a.

Scherk, 1975; Kauth and Thomas, 1976; Tucker and Maxwell, 1976; and Tucker, 1977).

The 16 cloud, cloud shadow, and high and low reflectance soil digital count measurements, the best fit linear line, and confidence bands about the linear line, using bands 5 and 7, are shown in Figure 1a. The numbers in the figure are Sun elevations in degrees. Since the origin is included within the dashed standard error of estimate lines, the intercept term (−0.01) of the best-fit line does not differ statistically from zero. Thus, MSS5 is approximately equal to 2.40MSS7. The 0 to 127 digital value range of MSS5 was twice as large as the 0 to 63 range for MSS7, which accounted for the factor 2 in the slope coefficient for MSS7. If the digital values of MSS7 are doubled, then MSS5 = 1.20MSS7.

Figure 1a indicates that Kauth's plane of soils in bands 5 and 7 is a family of overlapping soil brightness levels that can be extended to include clouds and cloud shadows along the best-fit line. The slope of this best-fit line (soil background line) appears constant from one overpass date to another, and the intercept term differs nonsignificantly from zero. Further investigations are needed to test conclusively whether the plane of soil shifts significantly from one study site to another or from one date to another. Possibly there is an effect on the bare soil line slope and intercept, because of atmospheric haze from scene to scene that will need to be studied further.

SUN ANGLE EFFECTS

Sun angle effects on bare soil reflectance are shown in Figure 1a. The Sun elevations for April 2, May 17, June 6, July 10, October 17, and December 10, 1975 (51, 57, 58, 56, 44, and 32°, respectively) are plotted for cloud (C), high reflecting soil (H), low reflecting soil (L), and shadow (S). In general, the greater the sun elevation the higher a point plots on the soil background line. For example, for the high reflecting soil sites, the Sun angle increased from 32° (12/10/75) to 56° (7/10/75) as the points labeled "H" progress up the line. The same correlation is true for low reflecting soil, even though there is some overlap with cloud shadows. The correlation breaks down slightly for clouds because the lowest C value is for 57° (5/17/75). On this date, the clouds were thin and wispy, and the cloud umbras were not very dense. Shadow or cloud umbra reflectance corresponded poorly with Sun angle, indicating that cloud translucence variations offset the sun angle effect.

COMPARING VEGETATION WITH SOIL BACKGROUND REFLECTANCE

Data (Table 3) collected on May 27, 1973, by the Landsat MSS, for sorghum fields with a range of LAI values from 3 to 9 (Richardson *et al.*, 1975), were plotted in Figure 1b for comparison with the 1975 soil background line. Each number represents the LAI values (rounded to one digit) measured for 10 sorghum fields plotted according to the mean digital data in MSS5 and MSS7. Data points for sorghum fields deviated perpendicularly from the bare soil background line. Furthermore, the sorghum fields with the larger LAI values, corresponding to increasing vegetation density, tended to be displaced furthest from the line. Thus, a measure of the distance of a candidate sorghum point from the line probably could be used as an index of the vegetation amount for that sorghum point. (Note: The Landsat digital counts may better characterize the fields than the LAI data because many LAI mea-

TABLE 3. MEAN DIGITAL DATA COLLECTED FROM TEN SORGHUM FIELDS ON MAY 27, 1973 (SCENE ID 1308-16323). AVERAGE ROW WIDTH WAS 97.6 CM. SUN ELEVATION WAS 62° AND SUN AZIMUTH WAS 93°. VEGETATION INDEXES FOR EIGHT VEGETATION INDEX (VI) MODEL TRANSFORMATIONS, TWO TRANSFORMED VI'S (TVI AND TVI6), RATIO VI (RVI), TWO PERPENDICULAR VI'S (PVI AND PVI6), DIFFERENCE VI (DVI), SOIL BRIGHTNESS INDEX (SBI), AND GREEN VI (GVI), DETERMINED FROM DIGITAL DATA FOR MSS4, MSS5, MSS6, AND MSS7, ARE LISTED. THE MSS DIGITAL DATA WERE CORRECTED FOR RADIANCE AND SUN ANGLE FOR CALCULATION OF TVI AND TVI6. THE ORIGINAL DIGITAL COUNT DATA WERE USED TO CALCULATE ALL OTHER TRANSFORMATIONS.

Landsat MSS Bands				Crop cover	Shadow cover	Plant height	Row azimuth	Leaf area	Vegetation Indice Transformations							
MSS4	MSS5	MSS6	MSS7	%	%	cm	°	index	TVI	TVI6	RVI	PVI	PVI6	DVI	SBI	GVI
38	33	46	34	75	8	75	82	3.0	0.85	0.78	0.97	19	9	49	15	73
48	47	58	34	35	5	45	81	3.9	0.75	0.74	1.38	13	9	35	11	93
38	31	56	30	90	10	110	1	4.1	0.84	0.85	1.03	16	18	42	20	77
38	28	58	29	80	20	110	1	4.2	0.85	0.89	0.97	16	22	42	22	76
43	41	53	26	65	1	60	91	4.2	0.70	0.75	1.58	8	9	22	9	82
39	32	56	31	65	9	85	81	4.9	0.84	0.84	1.03	16	17	43	20	78
33	24	60	37	70	30	85	3	5.1	0.95	0.94	0.65	25	26	66	31	74
34	24	65	40	90	5	110	89	6.9	0.97	0.95	0.60	28	29	73	35	79
37	27	67	40	85	15	100	3	7.3	0.94	0.93	0.68	27	29	70	34	83
36	28	65	38	90	2	110	91	8.5	0.93	0.92	0.74	24	27	64	31	81

surements are required to characterize a field precisely.)

Water deviates from the soil background line, but on the opposite side (Figure 1b) from vegetation. Candidate points (Table 1) representing water (W) are plotted in Figure 1b for April 2, July 10, October 17, and December 10, 1975 MSS data. The perpendicular distance of water from the bare soil line might help to improve water body monitoring techniques (Work and Gilmer, 1976). Work and Gilmer were trying to distinguish transition boundaries of water bodies and shore lines. A better knowledge of soil background reflectance also should benefit these kinds of investigations.

Sorghum data (Figure 2) collected on April 2, May 17, May 26, and June 4, 1975 by the Landsat MSS, for sorghum fields in dry and irrigated cropland areas with a range of LAI values from 1 to 8, were plotted as further evidence of the lateral deviation of vegetative MSS data from the soil background line (data set 2). The LAI ground truth was collected on May 6 and June 3, 1975 for dryland sorghum and on April 24 and May 24, 1975 for irrigated sorghum.

Figure 2a and b represent sorghum grown under dryland conditions in a year of low rainfall, when LAI was never very high; hence, points representing dryland sorghum fields never deviated very far from the soil background line. Figures 2c to 2f represent sorghum grown under irrigated conditions for various combinations of ground truth and MSS overpass dates, where LAI was higher, indicating greater sorghum plant vegetative growth; hence, points representing irrigated sorghum fields deviated further from the soil background line than did dryland sorghum fields.

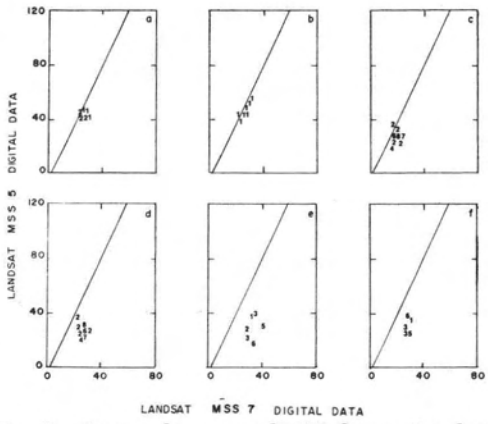

FIG. 2. Scatter diagrams of MSS data in Landsat bands 5 and 7 for sorghum fields grown under dry cropland conditions (a and b) and irrigated cropland conditions (c through f). Sorghum fields are identified by their LAI value rounded to one digit. Each figure is a different combination of MSS and ground truth (GT) data collection dates for 1975 as follows: (a) 5/17 and 5/6, (b) 6/4 and 6/3, (c) 4/2 and 4/24, (d) 5/17 and 4/24, (e) 5/26 and 5/24, and (f) 6/4 and 5/24, respectively.

VEGETATION INDEX MODELING

The soil background line could, perhaps, serve as a soil background reference for vegetation index (VI) modeling. Rouse *et al.* (1973) have developed two spectral VI models using Landsat MSS data that they used to compare multitemporal plant biomasses for several locations. Rouse's procedures involved an equation for correcting solar intensity (I_H) as a function of the solar constant (I_o) and sun elevation (α):

$$I_H = I_o \sin(\alpha), \tag{1}$$

and equations for determining two Transformed Vegetation Indexes (TVI and TVI6)

$$\text{TVI} = \sqrt{\frac{\text{MSS7} - \text{MSS5}}{\text{MSS7} + \text{MSS5}} + 0.5}\text{, and} \tag{2}$$

$$\text{TVI6} = \sqrt{\frac{\text{MSS6} - \text{MSS5}}{\text{MSS6} + \text{MSS5}} + 0.5}\,. \tag{3}$$

The MSS7+MSS5 and MSS6+MSS5 terms are "normalizing" terms while the 0.5 term is added to keep the TVI and TVI6 models from becoming negative (Deering *et al.*, 1975). The family of curves of Figure 3a indicates the range of values the TVI has for selected combinations of MSS5 and MSS7 values. The dashed line is the previously derived soil background line with a TVI value equal to 0.35.

A simple ratio of MSS5/MSS7 can be projected conically in Figure 3b as it was in Figure 3a. Thus, graphically a RVI=MSS5/MSS7 would have the same strengths and weaknesses as the TVI model. The RVI is simpler computationally than is the TVI. The dashed line is the soil background line using MSS bands 5 and 7 (Table 2); with a slope of 2.40.

Another VI model that could be used is the perpendicular distance of a vegetation candidate signature point from the soil background line as given by the equation:

$$\text{PVI} = \sqrt{(\text{Rgg5}-\text{Rp5})^2 + (\text{Rgg7}-\text{Rp7})^2}, \tag{4}$$

where,

PVI—is the perpendicular VI, defined as the perpendicular distance between the candidate vegetation point and the soil background line,

Rp—is the reflectance of a candidate vegetation point for Landsat bands MSS5 and MSS7, and

Rgg—is the reflectance of soil background corresponding to a candidate vegetation point.

A graphical interpretation of this equation is given in Figure 4 for bands MSS5 and MSS7. The soil background reflectance is interpreted as the intersection on the soil background line (Rgg5 and Rgg7) with a perpendicular drawn from a candidate signature point (Rp5, Rp7). The coordinates of this intersection on the soil background line, in terms of MSS5 and MSS7, can be found by solving the soil background general equation ($Rg5=a_0+a_1$ Rg7) and the vegetation general equation ($Rp5=b_0+b_1$ Rp7), that is perpendicular to the soil background equation, for the intersection coordinates (Rgg5, Rgg7) given by

$$\text{Rgg5} = \frac{b_1 a_0 - b_0 a_1}{b_1 - a_1}, \text{ and} \tag{5}$$

$$\text{Rgg7} = \frac{a_0 - b_0}{b_1 - a_1} \tag{6}$$

From Table 2, we determined that $a_1=2.40$ (slope of soil background line for MSS bands 5 and 7) and that a_0 does not differ statistically from zero (therefore, $a_0=0$). Also, since a_1 is perpendicular to b_1, then $b_1=-0.417$, so that $b_1-a_1=-2.82$. Substituting these values of a_0, a_1, and b_1 into Equations 5 and 6 yields $\text{Rgg5}=0.851b_0$ and $\text{Rgg7}=0.355b_0$. It can be shown from the vegetation perpendicular equation that $b_0=\text{Rp5}+0.417\text{Rp7}$, so that for any candidate vegetation signature, defined by the Landsat coordinates (Rp5, Rp7), the soil background reflectance coordinates are given by the equations:

$$\text{Rgg5} = 0.851\text{Rp5} + 0.355\text{Rp7}, \text{ and} \tag{7}$$

$$\text{Rgg7} = 0.355\text{Rp5} + 0.148\text{Rp7}. \tag{8}$$

Thus, once Rgg5 and Rgg7 are determined for a candidate vegetation measurement (Equations 7 and 8), then the PVI (Equation 4) can be computed as a spectral indicator of plant development or biomass accumulation. Figure 4 shows that PVI=0 indicates bare soil, a PVI<0 (negative) indicates water, and a PVI>0 (positive) indicates vegetation. A family of curves for selected combinations of MSS bands 5 and 7 values (Figure 5a) shows how the PVI is distributed in Landsat two-dimensional data space.

A computationally simpler method of

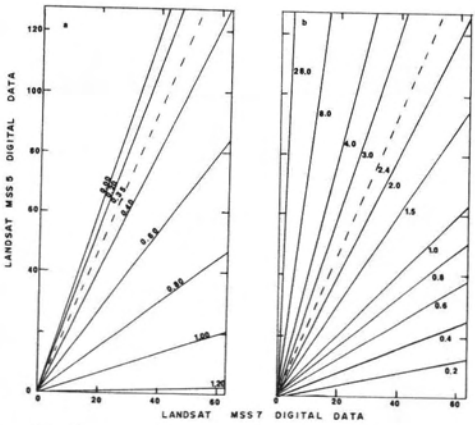

FIG. 3. Scatter diagrams showing distribution of (a) the Transformed Vegetation Index (TVI) and (b) Ratio Vegetation Index (RVI) in Landsat data space as defined by bands 5 and 7.

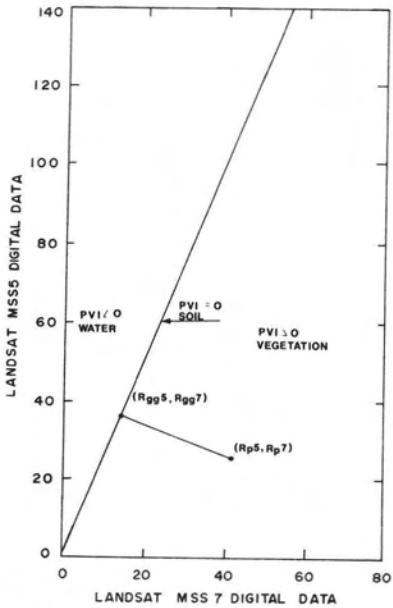

FIG. 4. Diagram illustrating principle of the perpendicular vegetation index (PVI) model. A perpendicular from candidate plant coordinates (Rp5, Rp7) intersects the soil background line at coordinates (Rgg5, Rgg7). As shown at PVI<0 (negative) indicates water, a PVI=0 indicates soil, and a PVI>0 (positive) indicates vegetation.

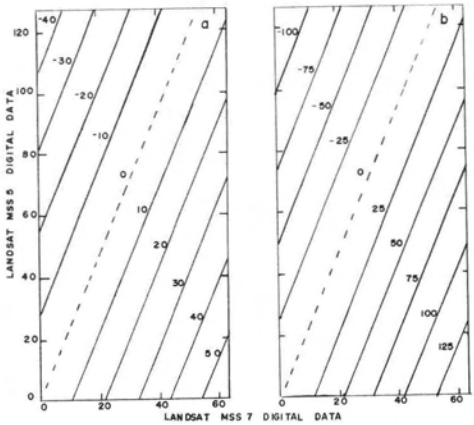

FIG. 5. Scatter diagrams showing distribution of (a) the Perpendicular Vegetation Index (PVI) and (b) the Differenced Vegetation Index (DVI) in Landsat data space as defined by bands 5 and 7.

achieving this same measure is to subtract MSS5 from MSS7 as given by

$$DVI = 2.40MSS7 - MSS5 \quad (9)$$

where DVI is the difference VI, and MSS7 is multiplied by the slope of the linear equation (Table 2) for the soil background line, defined by MSS bands 5 and 7. The graphical interpretation of the DVI in Figure 5b illustrates the correspondence to the PVI in Figure 5a. Figure 5b shows that a DVI=0 indicates bare soil, a DVI<0 (negative) indicates water, and a DVI>0 (positive) indicates vegetation. The disadvantage of this method is that the soil background coordinates (Rgg5, Rgg7) cannot be determined.

It is also possible to formulate another perpendicular distance vegetation index (PVI6) model, using bands 5 and 6 as follows:

$$PVI6 = \sqrt{(Rgg5-Rp5)^2 + (Rgg6-Rp6)^2}, \quad (10)$$

that is similar to the PVI model given by Equation 4. The bare soil intersection coordinates for this VI model were determined from the linear equation for bands 5 and 6, given in Table 2. Using the equation coefficients from Table 2, the bare soil intersection coordinates for the PVI6 model are given:

$$Rgg5 = -0.498 + 0.543Rp5 + 0.498Rp6, \quad (11)$$

and

$$Rgg6 = 2.734 + 0.498Rp5 + 0.457Rp6. \quad (12)$$

Kauth and Thomas (1976) have developed a technique for transforming the information contained in four-dimensional data space (i.e., defined by all 4 MSS bands) into a soil brightness index (SBI) and a green vegetation index (GVI). These transformations could be used as VI models using transformation coefficients given by Kauth as follows:

$$SBI = 0.433MSS4 + 0.632MSS5 + 0.586MSS6 + 0.264MSS7, \quad (13)$$

and

$$GVI = -0.290MSS4 - 0.562MSS5 + 0.600MSS6 + 0.491MSS7. \quad (14)$$

The SBI characterizes the soil background similar to the PVI and PVI6 soil background intersection coordinates. The GVI is a transformed VI.

Thus, we have described eight separate vegetation index models (TVI, TVI6, RVI, PVI, PVI6, DVI, SBI, and GVI) that could be used as indicators of vegetation density development. The PVI and PVI6 models permit calculation of the soil background intersection coordinates, (Rgg5, Rgg7) and (Rgg5, Rgg6) respectively, that we feel is an advantage over the other VI models because these intersection coordinates allow us to examine reasons (water content differences, shadows, tillage, soil crusting) for differences in reflectance of cropland, rangeland, and forest scenes due to soil background.

EVALUATION OF VEGETATION INDEXES

The simple correlation coefficients relating the eight VI models (TVI, TVI6, RVI, PVI, PVI6, DVI, SBI, and GVI) with four ground truth variables, crop cover, shadow cover, plant height, and leaf area index, are given in Table 4. The TVI, TVI6, and RVI models are used by Texas A&M University, College Station, Texas, as indicators of the amount and seasonal condition of rangeland vegetation (Deering *et al.*, 1975). The SBI and GVI are used in the Large Area Crop Inventory Experiment (LACIE) at the Johnson Spacecraft Center, Houston, Texas, for describing important crop phenomena concerning soil background and green development. The PVI, PVI6, and DVI models were developed in this report as indicators of vegetation development. Tucker (1977) has recently evaluated the RVI, TVI, and TVI6 models and has also found these transformations useful as indicators of vegetation amounts.

We found that the single channel correlations (r) of MSS5 with plant height

TABLE 4. SIMPLE LINEAR CORRELATION COEFFICIENTS BETWEEN EIGHT VEGETATION INDEX MODELS, BASED ON LANDSAT DIGITAL COUNT DATA COLLECTED FOR TEN SORGHUM FIELDS ON MAY 27, 1973, AND GROUND TRUTH INFORMATION FOR THE SAME FIELDS.

Vegetation Index Models	Ground truth information			
	Crop cover	Shadow cover	Plant height	Leaf area index
	correlation coefficients, r			
TVI	0.657*	0.446	0.717*	0.655*
TVI6	0.716*	0.466	0.828**	0.729*
RVI	−0.662*	−0.453	−0.733*	−0.630
PVI	0.565	0.324	0.596	0.723*
PVI6	0.681*	0.382	0.794**	0.812**
DVI	0.564	0.325	0.595	0.723*
GVI	0.662*	0.370	0.744*	0.808**
SBI	−0.621	−0.457	−0.539	0.132
LANDSAT MSS Bands	**Ground truth information**			
	Crop cover	Shadow cover	Plant height	Leaf area index
	correlation coefficients, r			
MSS4	−0.797**	−0.476	−0.773*	−0.482
MSS5	−0.809**	−0.518	−0.849**	−0.529
MSS6	0.342	0.124	0.502	0.877**
MSS7	0.295	0.137	0.314	0.702*

* Statistically significant at 0.05 probability level.
** Statistically significant at 0.01 probability level.

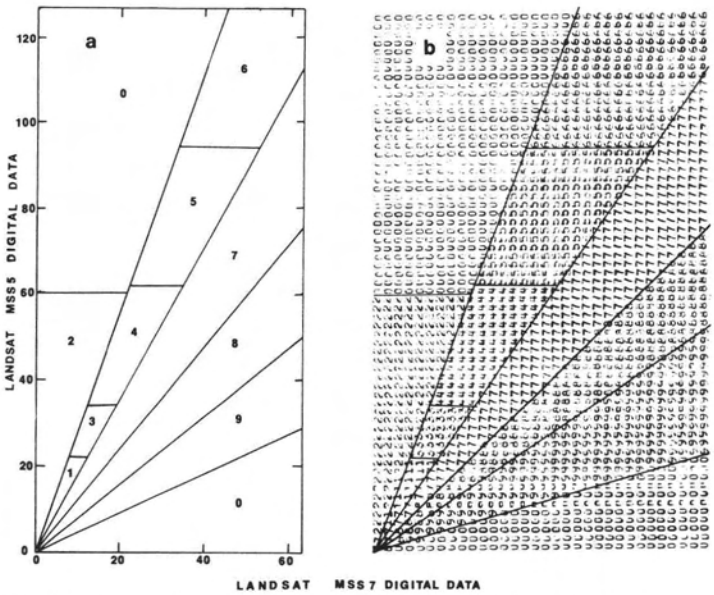

FIG. 6. Scatter diagram (a) shows the division of Landsat data space, defined by bands 5 and 7, into ten general crop and soil categories as follows: threshold (0), cloud shadow (6), water (2), low reflecting soil (3), medium reflecting soil (4), high reflecting soil (5), clouds (6), low vigor vegetation (7), medium vigor vegetation (8), and high vigor vegetation (9). Table lookup matrix (b) was devised to implement the division of Landsat data space from Figure 6a.

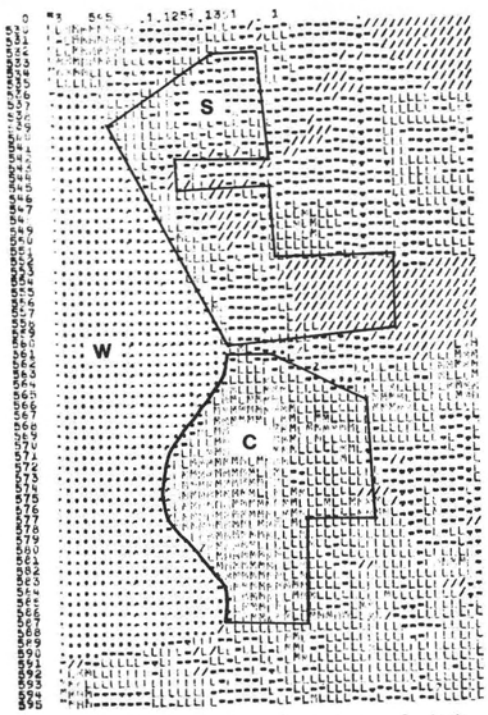

FIG. 7. Gray map printout of a water body (W), a sugarcane field (S), and citrus orchard (C), in Hidalgo County, Texas. The gray map is based on a table lookup technique that divides Landsat data space, defined by bands 5 and 7, into ten general crop and soil categories; threshold (T), water (·), cloud shadow (Z), low reflecting soil (−), medium reflecting soil (/), high reflecting soil (+), low cover vegetation (L), medium cover vegetation (M), and high cover vegetation (H). This gray map, corresponding to an April 2, 1975 Landsat overpass, delineates immature sugarcane with bare soil and low vegetation cover symbols. An established citrus orchard is delineated with low and medium vegetation cover symbols.

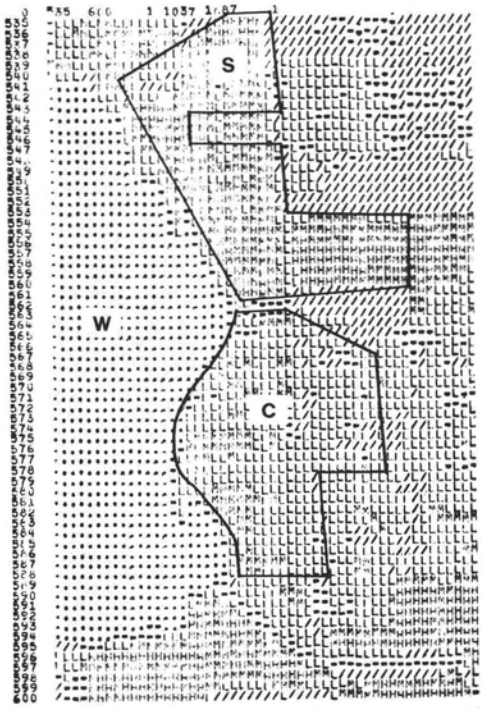

FIG. 8. The same symbology as for Figure 7, for a July 10, 1975 Landsat overpass. The rapidly growing sugarcane is delineated with low to high cover vegetation symbols, and the established citrus orchard is delineated with low to medium cover vegetation symbols.

(−0.849**) and MSS6 with leaf area index (0.877**) were higher than those produced by any of the VI models. The TVI6 model yielded the highest correlation with plant height (0.828**), while PVI6 correlated best with leaf area index (0.812**). Thus, these two VI models performed best, probably because of the high individual correlations of MSS5 and MSS6 with plant height and leaf area index, respectively.

As we expected, the SBI did not correlate significantly with any of the four ground truth parameters. The GVI was correlated significantly with crop cover (0.662*), plant height (0.744*), and leaf area index (0.808**).

Those VI models using Landsat MSS6 and not MSS7 (i.e., TVI6 and PVI6) correlated better with the ground truth information than the VI models that used MSS7 and not MSS6 (i.e., TVI, RVI, PVI, and DVI). Thus, for this set of ten sorghum fields, MSS6 contained more information about green vegetation development than did MSS7 (Tucker and Maxwell, 1976; Tucker, 1977). More testing is recommended with other sets of data to determine conclusively the superiority of MSS6 to MSS7 and TVI 6 and PVI6 models to TVI, RVI, PVI, and DVI models. Although individual Landsat bands may sometimes correlate better with yield than the VI models, the VI models provide better capability for temporal (season to season) comparisons of vegetation amounts and conditions.

IMPLICATIONS FOR MONITORING PLANT AND SOIL CONDITIONS

A gray mapping technique for displaying plant, soil, water, and cloud conditions for any Landsat overpass for any date for any study area location was devised as shown in Figure 6a and b. The Landsat data space, determined by bands MSS5 and MSS7, was arbitrarily divided into decision regions corresponding to ten general categories as shown in Figure 6a. These decision bound-

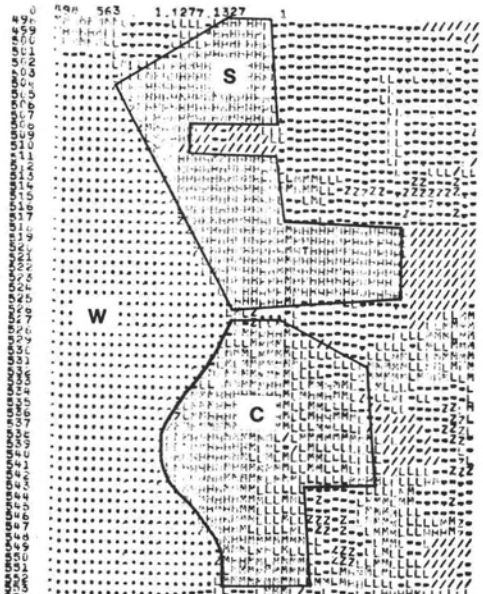

FIG. 9. The same symbology as for Figure 7, for an October 17, 1975 Landsat overpass. Mature sugarcane is delineated with high cover vegetation symbols while the established citrus orchard continues to be delineated with low to high cover vegetation symbols.

aries are a good first approximation for dividing Landsat data space. Kauth's line of soil is shown as an inverted cone with apex at the origin that can be considered as an expanding brightness scale composed of low (3), medium (4), and high (5) reflecting soil. The cone is terminated at the bottom by shadow (1) and is bounded at the top by the sensor saturation response for clouds (6). As Sun angle or illumination decreases, the range of soil reflectance decreases and the data are compressed toward the apex (origin) of the cone. Similarly, the variations of vegetation reflectance for low (7), medium (8), and high (9) vegetation cover follow conical paths that become narrower as Sun angle or illumination decreases. Water (2) is shown on the opposite side of the soil brightness scale from vegetation. The regions into which no data are expected to fall are called thresholds (0).

The construction of the decision boundaries among water, bare soil, and vegetation are fairly well known, based on the evidence presented in this paper. But the decision boundaries representing degrees of soil brightness and densities of vegetation cover will evolve as more applications and tests are made of them. Such categories can be expected to be "tuned" regionally for particular crops—like grain sorghum, wheat, and soybeans—and soil conditions. Tuning can also be expected among soils differing in productivity within a physiographic area or crop reporting distrct, and for irrigated versus nonirrigated crops in supplementally irrigated areas.

The decision boundaries of Figure 6a were implemented as a gray mapping process where the numbers, ranging from 0 to 9, were arranged in a table as indicated in Figure 6b. The candidate MSS5 and MSS7 signature pair is used as an address for the table in Figure 6b. The number at that specific address defines the signature category of the candidate signature pair. The process is repeated for each signature pair.

Figures 7 through 9 show the gray map results of crop, soil, and water conditions for a study site in Hidalgo County, Texas, using three of the six overpass dates, April 2, July 10, and October 17, 1975. The water body (·) is Delta Lake with two perennial crops, citrus and sugarcane, nearby. Using this gray mapping technique, the development of the sugarcane field could be monitored with respect to the citrus orchard during these three dates. In April (Figure 7), the citrus orchard is indicated by low (L) to medium (M) cover vegetation (gray map symbols). The sugarcane field is delineated by symbols indicating low (−) and medium(/) reflecting soil with some low cover vegetation, indicative of early season ratoon regrowth. By July (Figure 8), the sugarcane plants have developed considerably, so the sugarcane field is delineated by symbols indicating low to high cover vegetation as compared with low to medium cover vegetation in the citrus orchard. Finally, in October (Figure 9), the sugarcane is approaching maturity and is densely vegetated, while the citrus orchard is in a low to high vegetative cover condition.

The Sun elevation was 51, 56, and 44°, for April, July, and October, respectively, but the digital values for citrus and sugarcane were automatically referenced to bare soil brightness by using the table lookup procedure (Figures 6a and b). Thus, without any ground truth, the gray mapping technique allows delineation of any Landsat scene into vegetative cover stages, degrees of soil brightness, and water. The same technique can be used as a classification tool if ground truth is available for specifying meaningful vegetative cover categories or degrees of soil brightness for specific areas and dates.

Therefore, the techniques we describe can be used in rapid machine processing and classification procedures.

ACKNOWLEDGMENTS

We would like to thank A. H. Gerbermann, J. A. Cuellar, and E. J. Argueta for their work in collecting the ground truth data for sorghum used in this study.

REFERENCES

Allen, W. A., and A. J. Richardson. 1968. Interaction of light with a plant canopy. *Optical Soc. Amer.* 58(8):1023-1031.

Deering, D. W., J. W. Rouse, R. H. Haas, and J. A. Schell. 1975. Measuring "forage production" of grazing units from LANDSAT MSS data. *Proc. of the 10th Intl. Symp. on Remote Sens. of Environ.* II:1169-1178.

Kauth, R. J., and G. S. Thomas. 1976. The tasselled cap—A graphic description of the spectral-temporal development of agricultural crops as seen by LANDSAT. *Proc. Symp. Machine Proc. of Remote Sens. Data,* 6/29—7/2, LARS, Purdue, IEEE Cat. No. 76, Ch. 1103-1 MPRSD.

Kalensky, Z., and L. R. Scherk. 1975. Accuracy of forest mapping from LANDSAT computer compatible tapes. *Proc. of the 10th Intl. Symp. on Remote Sens. of Environ.* II:1159-1167.

Potter, J. F., and M. A. Mendlowitz. 1975. On the determination of haze levels from LANDSAT data. *Proc. of the 10th Intl. Symp. on Remote Sens. of Environ.* II:695-703.

Richardson, A. J., C. L. Wiegand, H. W. Gausman, J. A. Cuellar, A. H. Gerbermann. 1975. Plant, soil, and shadow components of row crops. *Photogrammetric Engineering and Remote Sensing,* November, 41(11):1401-1407.

Rouse, Jr., J. W., R. H. Hass, J. A. Schell, and D. W. Deering. 1973. Monitoring vegetation systems in the great plains with ERTS. *Third ERTS Symposium,* NASA SP-351. December 10-14, I:309-317.

Smith, J. A., R. E. Oliver, and O. E. Kalpela. 1973. Plant canopy models for simulating composite scene spectroradiance. *Remote Sens. of Earth Resources* (F. Shahrokhi, ed.), Space Institute, Univ. of Tennessee, Tullahoma, II:629-641.

Suits, G. H. 1971. The calculations of the directional reflectance of a vegetative canopy. *Remote Sens. of Environ.* 2:117-125.

Tucker, C. J. 1977. Use of near infrared/red radiance ratios for estimating vegetation biomass and physiological status. *Proc. of the 11th Intl. Symp. on Remote Sens. of Environ.* (In press).

Tucker, C. J., and E. L. Maxwell. 1976. Sensor design for monitoring vegetation canopies. *Photogrammetric Engineering and Remote Sensing.* 42(11):1399-1410.

Wiegand, C. L., H. W. Gausman, J. A. Cuellar, A. H. Gerbermann, and A. J. Richardson. 1974. Vegetation density as deduced from ERTS-1 MSS response. *Third ERTS Symp.,* NASA SP-351. December 10-14, I:93-116.

Work, E. A., and D. S. Gilmer. 1976. Utilization of satellite data for inventorying prairie ponds and lakes. *Photogrammetric Engineering and Remote Sensing.* 42(5):685-694.
